Canadian Journal of Physiology and Pharmacology

Article

Neonatal administration of fenofibrate had no developmental programming effect on the lipid profile and relative leucocyte telomere lengths of adolescent rats fed a high-fructose diet postnatally

Kasimu Ghandi Ibrahim[a,b,c], **Eliton Chivandi**[b], **Kennedy Honey Erlwanger**[b], **and Richard Leslie Brooksbank**[b]

[a]Department of Basic Medical and Dental Sciences, Faculty of Dentistry, Zarqa University, P.O. Box 2000, Zarqa 13110, Jordan; [b]School of Physiology, Faculty of Health Sciences, University of the Witwatersrand, 7 York Road, Parktown 2193, Johannesburg, South Africa; [c]Department of Physiology, Faculty of Basic Medical Sciences, College of Health Sciences, Usmanu Danfodiyo University, P.M.B. 2254, Sokoto, Nigeria

Corresponding author: **Kasimu Ghandi Ibrahim** (email: kibrahim@zu.edu.jo)

Abstract

Telomere length, a marker of ageing, is susceptible to developmental programming that may cause its accelerated attrition. Metabolic syndrome triggers telomere attrition. Fenofibrate, a peroxisome proliferator-activated receptor-alpha agonist, is protective against telomere attrition. We investigated the impact of fenofibrate administered during suckling on the lipid profile and leucocyte telomere lengths of rats fed a high-fructose diet post-weaning. Suckling Sprague-Dawley pups ($n = 119$) were allocated to four groups and gavaged with either 10 mL·kg^{-1} body mass 0.5% dimethyl sulfoxide, 100 mg·kg^{-1} body mass fenofibrate, fructose (20%, *w*/*v*), or a combination of fenofibrate and fructose for 15 days. Upon weaning, each of the initial groups was split into two subgroups: one had plain water while the other had fructose solution (20%, *w*/*v*) to drink for 6 weeks. Blood was collected for DNA extraction and relative leucocyte telomere length determination by real-time PCR. Plasma triglycerides and cholesterol were also quantified. The treatments had no effect ($p > 0.05$) on body mass, cholesterol concentration, and relative leucocyte telomere lengths in both sexes. Post-weaning fructose increased triglyceride concentrations ($p < 0.05$) in female rats. Fenofibrate administered during suckling did not affect ageing nor did it prevent high fructose-induced hypertriglyceridaemia in female rats.

Key words: telomere shortening, fenofibrate, metabolic syndrome, dyslipidaemia

Introduction

Dyslipidaemia, a cardinal feature of metabolic syndrome (MetS) (Iqbal et al. 2018), refers to an abnormality of lipoprotein metabolism resulting in either an overproduction of triglycerides and low-density lipoprotein (LDL) cholesterol or a deficiency of high-density lipoprotein (HDL) cholesterol (Berberich and Hegele 2022). Dyslipidaemia is not uncommon during pregnancy as it occurs consequent to the metabolic adjustments made by the body to ensure adequate foetal nutrition (Liberis et al. 2021).

The consumption of a high-fructose diet is a major driver of dyslipidaemia (Hieronimus and Stanhope 2020). The metabolism of fructose in the liver is not regulated like that of glucose. Hence, when fructose is phosphorylated to fructose-1-phosphate by fructokinase, some of it is converted to fatty acids, which eventually increase the circulating triacylglycerol levels and thus result in dyslipidaemia (Pepin et al. 2019).

Among several modalities of treatment, fenofibrate, a pregnancy class C drug, is used in the management of dyslipidaemia in pregnancy (Ahmed 2020). Pregnancy class C drugs, though beneficial, can cross the placental barrier and cause harmful effects on the growing foetus (Lewek and Banach 2022). Therefore, the beneficial effects of the use of drugs such as fenofibrate have to be weighed against their potential benefits.

Fenofibrate, a peroxisome proliferator-activated receptor alpha (PPAR-α) agonist, is used to treat dyslipidaemia (Mahmoudi et al. 2022). PPAR-α agonists modulate the metabolism of lipoproteins resulting in increased lipolysis especially of triglycerides and increase the clearance of low-density lipoproteins (Shah et al. 2010). At the molecular level, PPAR-α agonists modulate the activities of several regulatory genes in lipid and glucose metabolism, including those that decrease hepatic steatosis and inflammation (Han et al. 2018). Plasma lipid profile has been shown to significantly impact ageing, with dyslipidaemia being inversely related to

ageing (Johnson and Stolzing 2019). Moreover, lipid-lowering interventions have been shown to increase longevity (Huang et al. 2014).

Telomere length is used as a marker of chronological ageing and longevity (Teixeira 2021). In an *in vitro* model of telomere attrition under diabetes mellitus metabolic conditions using human dermal fibroblasts, fenofibrate counteracted the effects of dyslipidaemia and protected against telomere attrition (Sutanto et al. 2019). Telomeres, the repetitive non-coding sequences at the tips of the chromosomes (Chakravarti et al. 2021), serve many important functions including ensuring the stability of chromosomes during mitosis, preventing loss of genes, protecting DNA against damage, and preventing an end-to-end fusion of chromosomes (Wang and Wu 2021). As cells divide, the telomere length successively decreases due to incomplete replication of the lagging strand by the polymerase enzyme until it reaches a critical length at which point the cell can no longer divide (Grill and Nandakumar 2021). Telomere lengths show sexual dimorphism. Whereas men have been shown to have a faster telomere attrition rate (Dalgård et al. 2015), women have longer leucocyte telomere lengths due to the protective effects of oestrogen (Nawrot et al. 2004; Bekaert et al. 2007; Lulkiewicz et al. 2020).The leucocyte telomere length is a commonly used marker of chronological ageing in this respect (Bountziouka et al. 2022).

The telomere system comprising of telomeres and telomerase is mainly inherited (Vedder et al. 2021). However, stressor cues such as nutritional or pharmacological interventions during gestation and suckling, the early critical periods of developmental plasticity, can induce epigenetic changes in the form of DNA methylation and histone modification, which can then have an impact on the telomere system of the individual (van Lieshout et al. 2021). The suckling period in rodents, altricial mammals, is a critical window that has been targeted by researchers using drugs or natural compounds to program or reprogram for future metabolic health, including ageing (Reynolds et al. 2015). This practice of targeting the early periods of developmental plasticity to influence future metabolic health is called neonatal programming and buttresses the concept of developmental origins of health and disease (DOHaD) (Hsu and Tain 2021; Ibrahim et al. 2022).

In this study, we aimed to determine whether fenofibrate administered to rats during the suckling period would have an impact on the development of high-fructose diet-induced dyslipidaemia and telomere lengths of adolescent Sprague-Dawley rats.

Materials and methods

Study location and ethical clearance

The study was conducted at the Central Animal Services (CAS) Unit and the Laboratories at the School of Physiology, University of the Witwatersrand, Johannesburg, Republic of South Africa. All the protocols used in the study were approved by the Animal Ethics Screening Committee of the University of the Witwatersrand (certificate number: AESC/2016/04/18/B) and complied with international guidelines for the care and use of experimental animals as contained in the NRC guide for the Care and Use of Laboratory Animals: 8th Edition. The ARRIVE guidelines were used in the preparation of the manuscript.

Chemicals and reagents

All the chemicals and reagents used in the study were of analytical grade. Fenofibrate and dimethyl sulfoxide (DMSO) were supplied by Sigma–Aldrich (St. Louis, Missouri, USA). The fructose used was Nature's choice brand (Randvaal, South Africa). The real-time PCR reagents (SYBR™ Green Master Mix) were from Applied Biosystems, Thermo Fisher Scientific (Austin, TX, USA). The primers (telomeres and pyruvate kinase) and nuclease-free water used were from Inqaba Biotech (Pretoria, South Africa).

Animals, housing, and general care

A total of 119, 6-day-old suckling pups, littermates from 14 Sprague-Dawley dams were used in the study. The study was conducted in two phases: pre-weaning (postnatal days (PND) 6–21) and post-weaning (PND 22–63). In the pre-weaning phase, the pups were kept with their respective dams in the same cages and allowed to nurse freely. The cages were lined with wood shavings and shredded paper for environmental enrichment and changed twice weekly. At weaning, the dams were returned to the stock pool of CAS, while the weaned rats were transferred into individual cages. The ambient temperature of the room was kept at 26 ± 2 °C with adequate ventilation. A 12 h light cycle was maintained (lights on automatically at 07:00). The rats had ad libitum access to normal rat chow and drinking water or fructose as per their treatment protocol. The pups were weighed daily to adjust their treatment and ensure constant dosing in the first phase. Post-weaning, the rats were weighed twice weekly to monitor their growth and general health.

Study design

The study was carried out in two phases. In the pre-weaning phase, the pups were randomly allocated into four treatment groups in a split-litter manner and administered with either 0.5% DMSO (n = 29; males = 15, females = 14), 100 mg·kg^{-1} BW fenofibrate in 0.5% DMSO (n = 29; males = 15, females = 14), fructose solution 20% w/v in 0.5% DMSO (n = 29, males = 15, females = 14) or a combination of fenofibrate and fructose solution (n = 32; males = 16, females = 16). These treatments were administered at a volume of 10 mL·kg^{-1} BW, once daily (around 08:30–10:00) via oral gavage from PND 6 to PND 21. This phase of the study aimed to induce neonatal metabolic programming. Eight to twelve pups per dam were used to eliminate the effect of litter size.

The post-weaning phase of the study commenced on PND 22 with the weaning of the pups, their placement in individual cages, and the return of the dams to stock. All the pups had access to normal rat chow (Epol®, Centurion, South

Fig. 1. A schematic diagram summarizing the experimental design. DMSO, 10 mL·kg^{-1} of 0.5% dimethyl sulfoxide; FF, 100 mg·kg^{-1} fenofibrate; FW, fructose (20%, *w*/*v*); NRC, normal rat chow; TW, tap water; M, males; F, females.

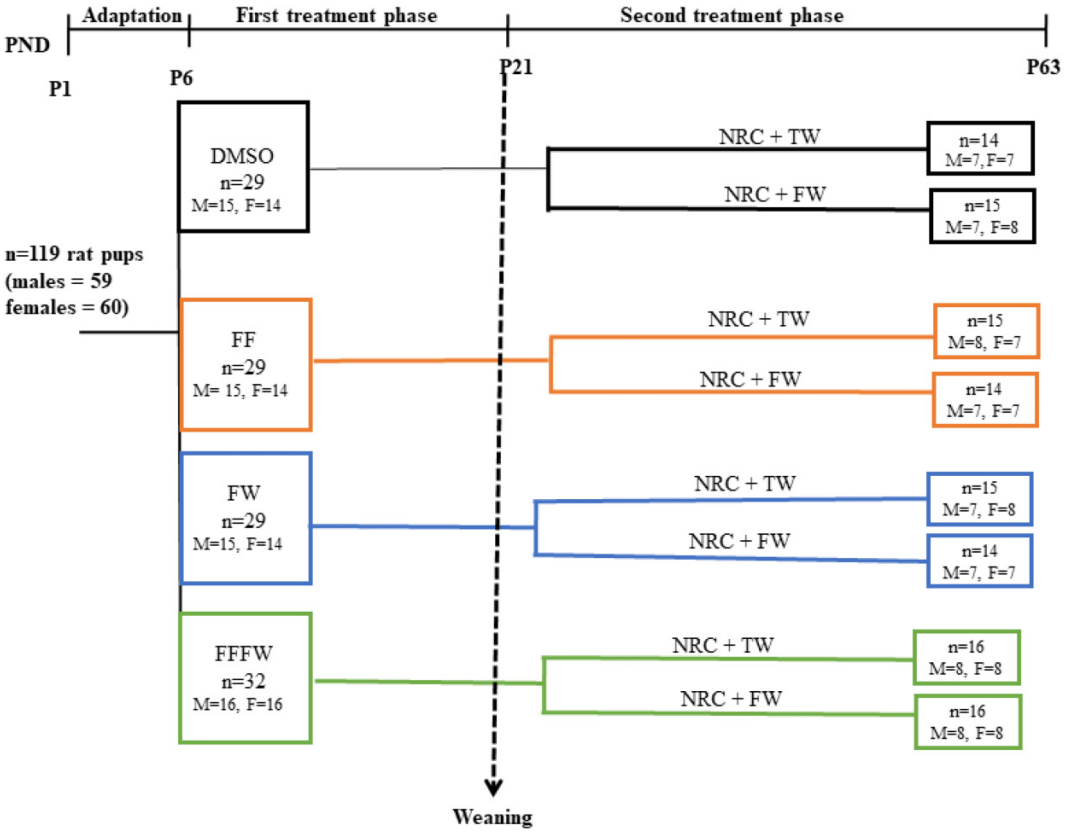

Africa), but each of the initial treatment groups was further subdivided into two based on their drinking fluid. One subgroup had access to plain tap water while the other had fructose, 20%, *w*/*v ad libitum* as their drinking fluid for 6 weeks until PND 63.

A schematic diagram summarizing the experimental design is shown in Fig. 1.

Terminal procedures

On PND 62, the rats were fasted overnight (with *ad libitum* acces to drinking water) and then on the morning of termination (PND 63), the body masses of the rats were determined with an electronic weighing scale (Snowrex Electronic Scale, Clover Scales, Johannesburg). The rats were then euthanized by an anaesthetic overdose using intraperitoneal sodium pentobarbitone (150 mg·kg^{-1} BW). Blood was taken via cardiac puncture and transferred into heparinised blood-collecting tubes (Becton Dickinson VACUTAINER Systems Europe, Meylan CEDEX, France). Genomic deoxyribonucleic acid (DNA) (DNA) was extracted from whole blood either immediately or when not possible, the blood was stored in a fridge till extraction (DEFY, Durban, South Africa) at 4 °C. Some of the blood was centrifuged (Hermle Z 230 A, B Hermle G, Germany) at 4000 × *g* at 4 °C for 15 min and the recovered plasma was pipetted into microtubes (Eppendorf, Germany) and stored at −20 °C until the determination of plasma lipids.

Determination of plasma concentration of cholesterol and triglycerides

The plasma cholesterol and triglycerides concentration were determined using a colorimetric analyser (IDEXX Catalyst Dx™ connected to an IDEXX Vet Lab station, IDEXX Laboratories Inc., Westbrook, Maine, USA).

Extraction of DNA

The whole blood collected at the termination of the rats was used to extract genomic DNA using the NucleoSpin Blood QuickPure kit (Macherey-Nagel, Düren, Germany) according to the manufacturer's instructions.

Determination of leucocyte telomere lengths

Leucocyte telomere lengths were determined by real-time quantitative polymerase chain reaction (RT-qPCR) using the StepOnePlus™ Real-Time PCR system (Applied Biosystems, Singapore). The detailed method used in carrying out the PCR has been previously described (Raymond et al. 2013; Ibrahim et al. 2019). In the present study, we determined the factor by which telomere repeat copy number (*T*) differed from the copy number of pyruvate kinase (*S*) (Cawthon 2002). The relative telomere length was expressed as the ratio of the telomere repeat copy number and the single gene copy number (*T*/*S*).

Statistical analysis

Data were analysed using the statistical software GraphPad Prism version 9.0 (GraphPad Software Inc., San Diego, CA) and expressed as mean ± standard error of the mean (SEM). A one-way Analysis of variance (ANOVA) was used to analyse the data, followed by a Bonferroni post hoc test to compare the means. The level of significance was set at $p < 0.05$.

Results

Figures 2A and 2B show the terminal body masses of male and female Sprague-Dawley rats that were administered with fenofibrate during suckling and fed a high-fructose diet post-weaning until adolescence. There were no differences ($p > 0.05$, ANOVA) in body masses observed across the treatment groups of both sexes.

The plasma concentrations of triglycerides in male and female Sprague-Dawley rats that were administered with fenofibrate as neonates and fed a high-fructose diet post-weaning till adolescence are presented in Figs. 3A and 3B.

There were no statistical differences ($p > 0.05$) among the treatment groups of the male rats. However, in the female rats, regardless of the treatment during suckling, a high-fructose diet post-weaning induced significantly higher ($p < 0.05$) plasma triglyceride concentration compared to female rats that drank plain tap water post-weaning.

Figures 4A and 4B show the plasma concentration of cholesterol of adolescent male and female Sprague-Dawley rats that were administered with fenofibrate during suckling followed by a high-fructose diet post-weaning.

The plasma cholesterol concentrations of the male and female Sprague-Dawley rats were similar ($p > 0.05$) across the treatment groups of both sexes.

The leucocyte telomere lengths of adolescent male and female Sprague-Dawley rats that were administered fenofibrate during suckling and then fed a high-fructose diet post-weaning till adolescence are presented in Figs. 5A and 5B.

The leucocyte telomere lengths of the rats were similar ($p > 0.05$) across the treatment groups in both male and female rats.

Discussion

The present study investigated the developmental programming effect of fenofibrate on some lipid profile parameters and leukocyte telomere length in adolescent rats following pre- and post-weaning exposure to a high-fructose diet. Both the neonatal and post-weaning interventions did not negatively affect the terminal body masses of the rats in this study. A high-fructose diet is known to induce obesity in rats (Pérez-Corredor et al. 2022). Given the rapid growth rate prior to adulthood in rats, it is expected that the rats in our study used most of the excess calories from the high-fructose diet for their growth. More so, it has been shown that neonatal obesogenic diets tend to only produce significant body mass changes around PND 100 (Patel and Srinivasan 2010). Of note, the rats in this study were terminated at PND 63, prior to

Fig. 2. (A) Terminal body masses of adolescent male Sprague-Dawley rats fed a high-fructose diet post-weaning. DMSO + TW = 10 mL·kg^{-1} of a 0.5% dimethyl sulfoxide solution as neonates and plain tap water post-weaning, DMSO + FW = 10 mL·kg^{-1} of a 0.5% dimethyl sulfoxide solution as neonates and fructose (20%, *w*/*v*) as drinking fluid post-weaning, FF + TW = fenofibrate (100 mg·kg^{-1} in 0.5% DMSO) as neonates and plain tap water post-weaning, FF + FW = fenofibrate (100 mg·kg^{-1} in 0.5% DMSO) as neonates and fructose (20%, *w*/*v*) as drinking fluid post-weaning, FW + TW = fructose (20%, *w*/*v*) as neonates and plain tap water post-weaning, FW + FW = fructose (20%, *w*/*v*) as neonates and fructose (20%, *w*/*v*) as drinking fluid post-weaning, FFFW + TW = fenofibrate (100 mg·kg^{-1}) and fructose (20%, *w*/*v*) in 0.5% DMSO as neonates and plain tap water post-weaning, and FFFW + FW = fenofibrate (100 mg·kg^{-1}) and fructose (20%, *w*/*v*) in 0.5% DMSO as neonates and fructose (20%, *w*/*v*) as drinking fluid post-weaning. Data expressed as mean ± SEM, n = 7–8 per group. (B) Terminal body masses of adolescent female Sprague-Dawley rats fed a high-fructose diet post-weaning. DMSO + TW = 10 mL·kg^{-1} of a 0.5% dimethyl sulfoxide solution as neonates and plain tap water post-weaning, DMSO + FW = 10 mL·kg^{-1} of a 0.5% dimethyl sulfoxide solution as neonates and fructose (20%, *w*/*v*) as drinking fluid post-weaning, FF + TW = fenofibrate (100 mg·kg^{-1} in 0.5% DMSO) as neonates and plain tap water post-weaning, FF + FW = fenofibrate (100 mg·kg^{-1} in 0.5% DMSO) as neonates and fructose (20%, *w*/*v*) as drinking fluid post-weaning, FW + TW = fructose (20%, *w*/*v*) as neonates and plain tap water post-weaning, FW + FW = fructose (20%, *w*/*v*) as neonates and fructose (20%, *w*/*v*) as drinking fluid post-weaning, FFFW + TW = fenofibrate (100 mg·kg^{-1}) and fructose (20%, *w*/*v*) in 0.5% DMSO as neonates and plain tap water post-weaning, and FFFW + FW = fenofibrate (100 mg·kg^{-1}) and fructose (20%, *w*/*v*) in 0.5% DMSO as neonates and fructose (20%, *w*/*v*) as drinking fluid post-weaning. Data are expressed as mean ± SEM, n = 7–8 per group.

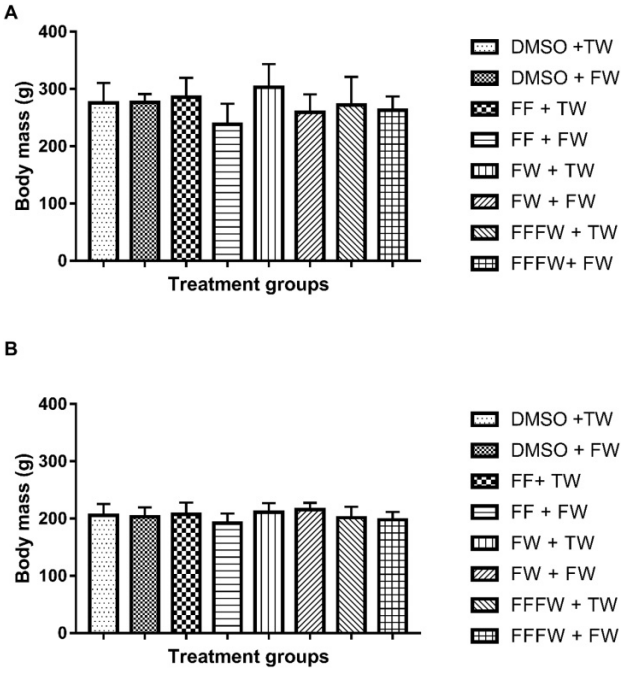

Fig. 3. (A) Plasma triglycerides concentration of adolescent male Sprague-Dawley rats fed a high-fructose diet post-weaning. DMSO + TW = 10 mL·kg^{-1} of a 0.5% dimethyl sulfoxide solution as neonates and plain tap water post-weaning, DMSO + FW = 10 mL·kg^{-1} of a 0.5% dimethyl sulfoxide solution as neonates and fructose (20%, *w*/*v*) as drinking fluid post-weaning, FF + TW = fenofibrate (100 mg·kg^{-1} in 0.5% DMSO) as neonates and plain tap water post-weaning, FF + FW = fenofibrate (100 mg·kg^{-1} in 0.5% DMSO) as neonates and fructose (20%, *w*/*v*) as drinking fluid post-weaning, FW + TW = fructose (20%, *w*/*v*) as neonates and plain tap water post-weaning, FW + FW = fructose (20%, *w*/*v*) as neonates and fructose (20%, *w*/*v*) as drinking fluid post-weaning, FFFW + TW = fenofibrate (100 mg·kg^{-1}) and fructose (20%, *w*/*v*) in 0.5% DMSO as neonates and plain tap water post-weaning, and FFFW + FW = fenofibrate (100 mg·kg^{-1}) and fructose (20%, *w*/*v*) in 0.5% DMSO as neonates and fructose (20%, *w*/*v*) as drinking fluid post-weaning. Data are expressed as mean ± SEM, n = 7–8 per group. (B) Plasma triglyceride concentration of adolescent female Sprague-Dawley rats fed a high-fructose diet post-weaning. $^{a, b}$ = significantly different at $p \leq 0.05$. DMSO + TW = 10 mL·kg^{-1} of a 0.5% dimethyl sulfoxide solution as neonates and plain tap water post-weaning, DMSO + FW = 10 mL·kg^{-1} of a 0.5% dimethyl sulfoxide solution as neonates and fructose (20%, *w*/*v*) as drinking fluid post-weaning, FF + TW = fenofibrate (100 mg·kg^{-1} in 0.5% DMSO) as neonates and plain tap water post-weaning, FF + FW = fenofibrate (100 mg·kg^{-1} in 0.5% DMSO) as neonates and fructose (20%, *w*/*v*) as drinking fluid post-weaning, FW + TW = fructose (20%, *w*/*v*) as neonates and plain tap water post-weaning, FW + FW = fructose (20%, *w*/*v*) as neonates and fructose (20%, *w*/*v*) as drinking fluid post-weaning, FFFW + TW = fenofibrate (100 mg·kg^{-1}) and fructose (20%, *w*/*v*) in 0.5% DMSO as neonates and plain tap water post-weaning, and FFFW + FW = fenofibrate (100 mg·kg^{-1}) and fructose (20%, *w*/*v*) in 0.5% DMSO as neonates and fructose (20%, *w*/*v*) as drinking fluid post-weaning. Data are expressed as mean ± SEM, n = 7–8 per group.

Fig. 4. (A) Plasma cholesterol concentration of adolescent male Sprague-Dawley rats fed a high-fructose diet post-weaning. DMSO + TW = 10 mL·kg^{-1} of a 0.5% dimethyl sulfoxide solution as neonates and plain tap water post-weaning, DMSO + FW = 10 mL·kg^{-1} of a 0.5% dimethyl sulfoxide solution as neonates and fructose (20%, *w*/*v*) as drinking fluid post-weaning, FF + TW = fenofibrate (100 mg·kg^{-1} in 0.5% DMSO) as neonates and plain tap water post-weaning, FF + FW = fenofibrate (100 mg·kg^{-1} in 0.5% DMSO) as neonates and fructose (20%, *w*/*v*) as drinking fluid post-weaning, FW + TW = fructose (20%, *w*/*v*) as neonates and plain tap water post-weaning, FW + FW = fructose (20%, *w*/*v*) as neonates and fructose (20%, *w*/*v*) as drinking fluid post-weaning, FFFW + TW = fenofibrate (100 mg·kg^{-1}) and fructose (20%, *w*/*v*) in 0.5% DMSO as neonates and plain tap water post-weaning, FFFW + FW = fenofibrate (100 mg·kg^{-1}) and fructose (20%, *w*/*v*) in 0.5% DMSO as neonates and fructose (20%, *w*/*v*) as drinking fluid post-weaning. Data are expressed as mean ± SEM, n = 7–8 per group. (B) Plasma cholesterol concentration of adolescent female Sprague-Dawley rats fed a high-fructose diet post-weaning. DMSO + TW = 10 mL·kg^{-1} of a 0.5% dimethyl sulfoxide solution as neonates and plain tap water post-weaning, DMSO + FW = 10 mL·kg^{-1} of a 0.5% dimethyl sulfoxide solution as neonates and fructose (20%, *w*/*v*) as drinking fluid post-weaning, FF + TW = fenofibrate (100 mg·kg^{-1} in 0.5% DMSO) as neonates and plain tap water post-weaning, FF + FW = fenofibrate (100 mg·kg^{-1} in 0.5% DMSO) as neonates and fructose (20%, *w*/*v*) as drinking fluid post-weaning, FW + TW = fructose (20%, *w*/*v*) as neonates and plain tap water post-weaning, FW + FW = fructose (20%, *w*/*v*) as neonates and fructose (20%, *w*/*v*) as drinking fluid post-weaning, FFFW + TW = fenofibrate (100 mg·kg^{-1}) and fructose (20%, *w*/*v*) in 0.5% DMSO as neonates and plain tap water post-weaning, and FFFW + FW = fenofibrate (100 mg·kg^{-1}) and fructose (20%, *w*/*v*) in 0.5% DMSO as neonates and fructose (20%, *w*/*v*) as drinking fluid post-weaning. Data expressed as mean ± SEM, n = 7–8 per group.

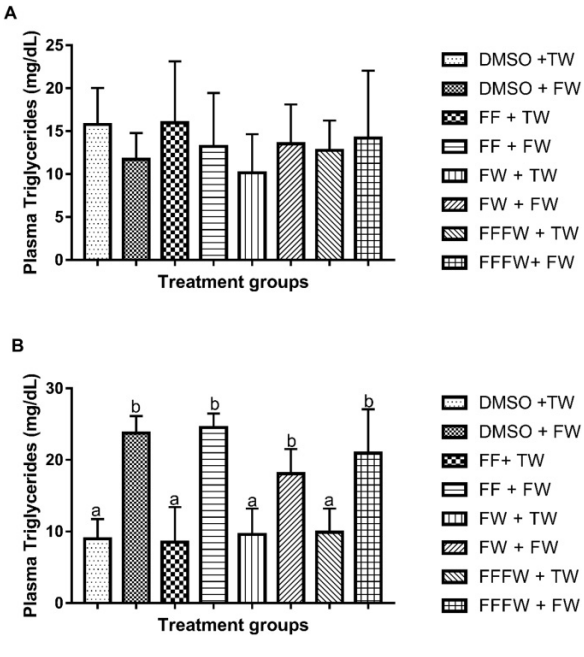

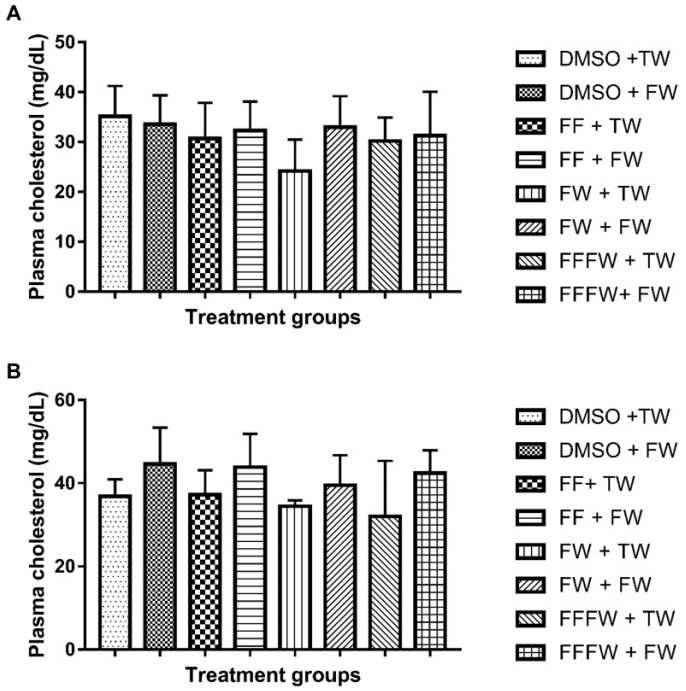

Fig. 5. (A) Leucocyte telomere length of adolescent male Sprague-Dawley rats fed a high-fructose diet post-weaning. DMSO + TW = 10 mL·kg^{-1} of a 0.5% dimethyl sulfoxide solution as neonates and plain tap water post-weaning, DMSO + FW = 10 mL·kg^{-1} of a 0.5% dimethyl sulfoxide solution as neonates and fructose (20%, *w*/*v*) as drinking fluid post-weaning, FF + TW = fenofibrate (100 mg·kg^{-1} in 0.5% DMSO) as neonates and plain tap water post-weaning, FF + FW = fenofibrate (100 mg·kg^{-1} in 0.5% DMSO) as neonates and fructose (20%, *w*/*v*) as drinking fluid post-weaning, FW + TW = fructose (20%, *w*/*v*) as neonates and plain tap water post-weaning, FW + FW = fructose (20%, *w*/*v*) as neonates and fructose (20%, *w*/*v*) as drinking fluid post-weaning, FFFW + TW = fenofibrate (100 mg·kg^{-1}) and fructose (20%, *w*/*v*) in 0.5% DMSO as neonates and plain tap water post-weaning, FFFW + FW = fenofibrate (100 mg·kg^{-1}) and fructose (20%, *w*/*v*) in 0.5% DMSO as neonates and fructose (20%, *w*/*v*) as drinking fluid post-weaning. Data are expressed as mean ± SEM, n = 7–8 per group. (B) Leucocyte telomere length of adolescent female Sprague-Dawley rats fed a high-fructose diet post-weaning. DMSO + TW = 10 mL·kg^{-1} of a 0.5% dimethyl sulfoxide solution as neonates and plain tap water post-weaning, DMSO + FW = 10 mL·kg^{-1} of a 0.5% dimethyl sulfoxide solution as neonates and fructose (20%, *w*/*v*) as drinking fluid post-weaning, FF + TW = fenofibrate (100 mg·kg^{-1} in 0.5% DMSO) as neonates and plain tap water post-weaning, FF + FW = fenofibrate (100 mg·kg^{-1} in 0.5% DMSO) as neonates and fructose (20%, *w*/*v*) as drinking fluid post-weaning, FW + TW = fructose (20%, *w*/*v*) as neonates and plain tap water post-weaning, FW + FW = fructose (20%, *w*/*v*) as neonates and fructose (20%, *w*/*v*) as drinking fluid post-weaning, FFFW + TW = fenofibrate (100 mg·kg^{-1}) and fructose (20%, *w*/*v*) in 0.5% DMSO as neonates and plain tap water post-weaning, and FFFW + FW = fenofibrate (100 mg·kg^{-1}) and fructose (20%, *w*/*v*) in 0.5% DMSO as neonates and fructose (20%, *w*/*v*) as drinking fluid post-weaning. Data are expressed as mean ± SEM, n = 7–8 per group.

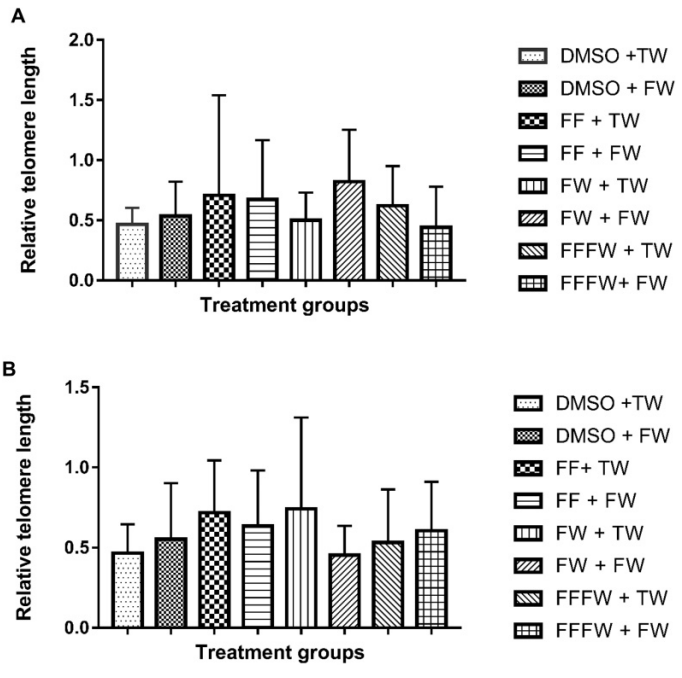

the adolescent surge in sex hormones responsible for weight gain.

Furthermore, our results indicate that postnatal high-fructose feeding induces hypertriglyceridaemia in female rats. This high-fructose diet-induced hypertriglyceridaemia was not prevented by an earlier fenofibrate administration during suckling. Thus, fenofibrate did not exhibit prophylactic potential in preventing hypertriglyceridaemia in the female rats and may therefore not be an ideal candidate for neonatal programming against later-life dyslipidaemia. Consumption of high-fructose diets is known to induce de novo lipogenesis (DNL) by stimulating excess production of triglycerides in both the liver and the small intestines (Le et al. 2009; Zhao et al. 2020) Fructose activates the carbohydrate-responsive-element-binding protein (ChERBP) and consequently upregulates the microsomal triglyceride transfer protein (MTTP) (Erion et al. 2013). MTTP is an important enzyme in the packaging of triglycerides in both the liver as very low-density lipoproteins and in the intestines as chylomicrons (Wallace and Metallo 2020).

Fenofibrate as a PPAR α agonist acts primarily in the liver and inhibits DNL through oxidation of hepatic lipids and hence decreases the concentration of triacylglycerol (Mahmoudi et al. 2022), and also, via enhancing glycaemic status, decreases oxidative stress and increases antioxidant status (Abdelmoneim et al. 2021). However, in our study where fenofibrate was administered prophylactically in the neonatal stage prior to fructose administration, it did not prevent fructose-induced hypertriglyceridaemia in the female rats. This suggests that fenofibrate may not be a good candidate for programming against dyslipidaemia in females.

In addition, the high-fructose diet did not significantly induce hypertriglyceridaemia in the male rats. This is not surprising as previous studies have already established sexual dimorphism in susceptibility to high-fructose diet-induced changes (Fuente-Martín et al. 2012; Stephenson et al. 2022). It is well known that females are more responsive to the ingestion of high-fructose diets and hence DNL than males (Low et al. 2018). Studies have revealed a sexually dimorphic pattern in fat distribution, with males storing more lipids in the viscera and females in the peripheral adipose tissues (Chen et al. 2022). Oestrogen is thought to inhibit peripheral lipolysis of subcutaneous fat in females without affecting the visceral fat mass (Pedersen et al. 2004). Sexual dimorphism also exists in the differential storage of lipids in the liver and in the skeletal muscles. It has been previously shown that females tend to store more lipids in the muscles as compared to males that store more lipids in the liver (Høeg et al. 2009; Beaudry and Devries 2019). It is, therefore, not surprising to find a sex difference in the fructose-induced hypertriglyceridaemia found in the current study.

In addition, the total plasma cholesterol concentration was not affected by both the neonatal and post-weaning interventions in both male and female rats. This finding was unexpected, as consumption of a high-fructose diet has been associated with hypercholesterolaemia (Lê et al. 2009; Koo et al. 2021). However, we found a few studies where the consumption of a high-fructose diet did not induce hypercholesterolaemia in rats (Muhammad et al. 2020; Iskender et al. 2022).

We speculate that, as with the body mass gain, the growing rats used up most of the excess calories for their growth and hyperactivity.

Lastly, neonatal-administered fenofibrate did not have any impact on the leucocyte telomere lengths of the adolescent rats. Neonatal programming is usually a result of epigenetic changes that occur during the early critical developmental periods that then modulate the expression of metabolic genes and permanently alter the physiology of the individual (Xargay-Torrent et al. 2022). DNA methylation, which involves the addition of a methyl group to the DNA, is an important epigenetic phenomenon that influences the transcription and expression or repression of genes (Wong 2021). This DNA methylation, facilitated by the DNA methyl transferase (DNMT), forms a stable epigenetic mark that can be transmitted to subsequent generations without having to repeat the initial insult (Zhu et al. 2019). To this end, previous studies have shown fenofibrate to be a good candidate for neonatal programming because of its ability to downregulate the epigenetic enzyme, DNMT-1 (Kong et al. 2021). This implies that fenofibrate could be of potentially immense benefit in slowing down ageing later in life when used during the critical developmental periods of gestation and suckling. To further support this idea, fenofibrate was shown to protect telomeres against attrition in an in vitro study using human dermal fibroblasts under diabetic conditions through yet-to-be-understood mechanisms (Sutanto et al. 2019).

In the present study, both fenofibrate and fructose were administered during suckling to induce programming. The potential impact of these interventions on the telomere length is quite high. This is because it is thought that telomere lengths are determined in the hematopoietic stem cells in the bone marrow. These stem cells usually develop and reach maturity in the 6th week of gestation (Mikkola and Orkin 2006). Our intervention in the suckling phase was appropriate as the critical window usually extends through suckling to early childhood (Hochberg et al. 2011). Interestingly, studies have reported differences in telomere lengths early in life and in adolescence following interventions during gestation in humans. Prenatal smoking of cigarettes by mothers was shown to result in shorter telomeres in 196 children under the age of 15 years in a study in Hong Kong (Ip et al. 2016). Additionally, Latino children who were exclusively breastfed for 4–6 weeks after birth were shown to have longer telomere lengths at 4–5 years compared to their colleagues who were not exclusively breastfed (Wojcicki et al. 2016). We expected to see changes in the telomere lengths of the rats in this study as they were terminated at PND 63, which corresponds to late adolescence in man (Andreollo et al. 2012). However, we did not find any such correlation. It should be noted that similar to our findings, some studies have challenged this correlation between early interventions and telomere lengths. In our laboratory, for instance, we did not find any impact on the telomere lengths of adolescent rats that were administered with curcumin and fructose during suckling (Ibrahim et al. 2019). In another study, maternal homocysteine levels, though related to cigarette smoking did not show any significant correlation with foetal telomere lengths (Tellechea et al. 2015). These seemingly contrasting scenarios buttress the imperative of further research in the area of telomere biology as it relates to neonatal programming to enhance our understanding.

In this study, we did not quantify the feed and fluid intake of the rats, especially the amount of fructose taken and the percentage of caloric intake it represents. This could have provided some insights into the differential response between the male and the female rats in the fructose-induced plasma triglyceride concentration. However, it has been previously shown that female rats had more preference for sugar, thereby consuming proportionately more and increasing their caloric intake than their male counterparts (Sclafani et al. 1987).

Conclusion

Neonatal programming with fenofibrate did not have an impact on the development of hypertriglyceridaemia in females when they consumed a high-fructose diet later in life. Additionally, it did not alter ageing as measured by leucocyte telomere length in male and female rats. Thus, fenofibrate may not be an ideal candidate for neonatal programming against dyslipidaemia and telomere attrition.

Article information

History dates

Received: 14 November 2022
Accepted: 26 June 2023
Accepted manuscript online: 11 July 2023
Version of record online: 4 September 2023

Copyright

Data availability

Data generated or analysed during this study are provided in full within the published article.

Author information

Author ORCIDs

Kasimu Ghandi Ibrahim https://orcid.org/0000-0002-2119-580X

Author contributions

Conceptualization: IGK, KHE
Data curation: IGK, EC
Formal analysis: IGK, EC
Funding acquisition: IGK, KHE
Investigation: IGK, RLB
Methodology: IGK, EC, KHE, RLB
Project administration: KHE, RLB
Supervision: EC, KHE, RLB
Validation: EC, KHE
Writing – original draft: IGK
Writing – review & editing: IGK, EC, KHE, RLB

Competing interests

The authors declare there are no competing interests.

Funding information

This study received grants from the Faculty of Health Sciences Research Committee of the University of the Witwatersrand, Johannesburg (KGI, Grant number: 001.251.8521101.5121105.000000.0000000000.4550) and the National Research Foundation of South Africa (KHE, Grant number: IRF 2010041900009).

References

Abdelmoneim, D., El-Adl, M., El-Sayed, G., and El-Sherbini, E.S. 2021. Protective effect of fenofibrate against high-fat–high-fructose diet induced non-obese NAFLD in rats. Fundam. Clin. Pharmacol. **35**: 379–388. doi:10.1111/fcp.12597.

Ahmed, S.S. 2020. An update on pharmacotherapy of dyslipidemia for adults. J. Adv. Med. Med. Res. **32**: 86–109. doi:10.9734/jammr/2020/v32i830469.

Andreollo, N.A., Santos, E.F.D., Araújo, M.R., and Lopes, L.R. 2012. Rat's age versus human's age: What is the relationship? *ABCD*. Arq. Bras. Cir. Dig. **25**: 49–51. doi:10.1590/SO102-67202012000100011.

Beaudry, K.M., and Devries, M.C. 2019. Sex-based differences in hepatic and skeletal muscle triglyceride storage and metabolism. Appl. Physiol. Nutr. Metab. **44**: 805–813. doi:10.1139/apnm-2018-0635.

Bekaert, S., De Meyer, T., Rietzschel, E.R., De Buyzere, M.L., De Bacquer, D., Langlois, M., et al. 2007. Telomere length and cardiovascular risk factors in a middle-aged population free of overt cardiovascular disease. Aging Cell, **6**: 639–647. doi:10.1111/j.1474-9726.2007.00321.x. PMID: 17874998.

Berberich, A.J., and Hegele, R.A. 2022. A modern approach to dyslipidemia. Endocr. Rev. **43**: 611–653. doi:10.1210/endrev/bnab037.

Bountziouka, V., Nelson, C.P., Codd, V., Wang, Q., Musicha, C., Allara, E., et al. 2022. Association of shorter leucocyte telomere length with risk of frailty. J. Cachexia Sarcopenia Muscle, **13**: 1741–1751. doi:10.1002/jcsm.12971. PMID: 35297226.

Cawthon, R.M. 2002. Telomere measurement by quantitative PCR. Nucleic Acids Res. **30**: e47–e47. doi:10.1093/nar/30.10.e47. PMID: 12000852.

Chakravarti, D., Labella, K.A., and Depinho, R.A. 2021. Telomeres: history, health, and hallmarks of aging. Cell, **184**: 306–322. doi:10.1016/j.cell.2020.12.028. PMID: 33450206.

Chen, X.-Y., Wang, C., Huang, Y.-Z., and Zhang, L.-L. 2022. Nonalcoholic fatty liver disease shows significant sex dimorphism. World J. Clin. Cases, **10**: 1457–1472. doi:10.12998/wjcc.v10.i5.1457. PMID: 35211584.

Dalgård, C., Benetos, A., Verhulst, S., Labat, C., Kark, J.D., Christensen, K., et al. 2015. Leukocyte telomere length dynamics in women and men: menopause vs age effects. Int. J. Epidemiol., **44**: 1688–1695. doi:10.1093/ije/dyv165. PMID: 26385867.

Erion, D.M., Popov, V., Hsiao, J.J., Vatner, D., Mitchell, K., Yonemitsu, S., et al. 2013. The role of the carbohydrate response element-binding protein in male fructose-fed rats. Endocrinology, **154**: 36–44. doi:10.1210/en.2012-1725. PMID: 23161873.

Fuente-Martín, E., Granado, M., García-Cáceres, C., Sanchez-Garrido, M.A., Frago, L.M., Tena-Sempere, M., et al. 2012. Early nutritional changes induce sexually dimorphic long-term effects on body weight gain and the response to sucrose intake in adult rats. Metabolism, **61**: 812–822. doi:10.1016/j.metabol.2011.11.003. PMID: 22209665.

Grill, S., and Nandakumar, J. 2021. Molecular mechanisms of telomere biology disorders. J. Biol. Chem. **296**: 10064. doi:10.1074/jbc.REV120.014017.

Han, J.S., Kim, K., Jung, Y., Lee, J.-H., Namgung, J., Lee, H.-Y., et al. 2018. Metabolic alterations associated with atorvastatin/fenofibric acid combination in patients with atherogenic dyslipidaemia: a randomized trial for comparison with escalated-dose atorvastatin. Sci. Rep. **8**: 1–10. doi:10.1038/s41598-018-33058-x. PMID: 29311619.

Hieronimus, B., and Stanhope, K.L. 2020. Dietary fructose and dyslipidemia: new mechanisms involving apoC3. Curr. Opin. Lipidol. **31**: 20–26. doi:10.1097/MOL.0000000000000653. PMID: 31789670.

Hochberg, Z.E., Feil, R., Constancia, M., Fraga, M., Junien, C., Carel, J.-C., et al. 2011. Child health, developmental plasticity, and epigenetic programming. Endocr. Rev. **32**: 159–224. doi:10.1210/er.2009-0039. PMID: 20971919.

Høeg, L., Roepstorff, C., Thiele, M., Richter, E.A., Wojtaszewski, J.F., and Kiens, B. 2009. Higher intramuscular triacylglycerol in women does not impair insulin sensitivity and proximal insulin signaling. J. Appl. Physiol. **107**: 824–831. doi:10.1152/japplphysiol.91382.2008. PMID: 19574502.

Hsu, C.-N., and Tain, Y.-L. 2021. Animal models for DOHaD research: focus on hypertension of developmental origins. Biomedicines, **9**: 623. doi:10.3390/biomedicines9060623. PMID: 34072634.

Huang, X., Withers, B.R., and Dickson, R.C. 2014. Sphingolipids and lifespan regulation. Biochim. Biophys. Acta. **1841**: 657–664. doi:10.1016/j.bbalip.2013.08.006.

Ibrahim, K.G., Chivandi, E., Erlwanger, K.H., and Brooksbank, R.L. 2019. Neonatal oral curcumin: effect on telomere lengths of adolescent rats fed a high fructose diet post-weaning. J. Biol. Sci. **19**: 224–230. doi:10.3923/jbs.2019.224.230.

Ibrahim, K.G., Usman, D., Bello, M.B., Malami, I., Abubakar, B., Abubakar, M.B., and Imam, M.U. 2022. Rodent models of metabolic disorders: considerations for use in studies of neonatal programming. Br. J. Nutr. **128**: 802–827. doi:10.1017/S0007114521003834. PMID: 34551828.

Ip, P., Chung, B.H.Y., Ho, F.K.W., Chan, G.C.F., Deng, W., Wong, W.H.S., et al. 2016. Prenatal tobacco exposure shortens telomere length in children. Nicotin Tob. Res. **19**: 111–118. doi:10.1093/ntr/ntw139.

Iqbal, J., Al Qarni, A., Hawwari, A., Alghanem, A.F., and Ahmed, G. 2018. Metabolic syndrome, dyslipidemia and regulation of lipoprotein metabolism. Curr. Diabetes Rev. **14**: 427–433. doi:10.2174/1573399813666170705161039. PMID: 28677496.

Iskender, H., Yenice, G., Terim Kapakin, K.A., Dokumacioglu, E., Sevim, C., Hayirli, A., and Altun, S. 2022. Effects of high fructose diet on lipid metabolism and the hepatic NF-κb/SIRT-1 pathway. Biotech. Histochem. **97**: 30–38. doi:10.1080/10520295.2021.1890214.

Johnson, A.A., and Stolzing, A. 2019. The role of lipid metabolism in aging, lifespan regulation, and age-related disease. Aging Cell, **18**: e13048. doi:10.1111/acel.13048. PMID: 31560163.

Kong, R., Wang, N., Han, W., Bao, W., and Lu, J. 2021. Fenofibrate exerts antitumor effects in colon cancer via regulation of DNMT1 and CDKN2A. PPAR Res. **2021**, Article ID 6663782|. doi:10.1155/2021/6663782.

Koo, S., Kim, M., Cho, H.M., and Kim, I. 2021. Maternal high-fructose intake during pregnancy and lactation induces metabolic syndrome in adult offspring. Nutr. Res. Pract. **15**: 160–172. doi:10.4162/nrp.2021.15.2.160. PMID: 33841721.

Lê, K.-A., Ith, M., Kreis, R., Faeh, D., Bortolotti, M., Tran, C., et al. 2009. Fructose overconsumption causes dyslipidemia and ectopic lipid deposition in healthy subjects with and without a family history of type 2 diabetes. Am. J. Clin. Nutr. **89**: 1760–1765. doi:10.3945/ajcn.2008.27336. PMID: 19403641.

Lewek, J., and Banach, M. 2022. Dyslipidemia management in pregnancy: Why is it not covered in the guidelines? Curr. Atheroscler. Rep. **24**: 547–556. doi:10.1007/s11883-022-01030-w. PMID: 35499807.

Liberis, A., Petousis, S., and Tsikouras, P. 2021. Lipid disorders in pregnancy. Curr. Pharm. Des. **27**: 3804–3807. doi:10.2174/1381612827666210421103245. PMID: 33882801.

Low, W.S., Cornfield, T., Charlton, C.A., Tomlinson, J.W., and Hodson, L. 2018. Sex differences in hepatic de novo lipogenesis with acute fructose feeding. Nutrients, **10**: 1263. doi:10.3390/nu10091263. PMID: 30205493.

Lulkiewicz, M., Bajsert, J., Kopczynski, P., Barczak, W., and Rubis, B. 2020. Telomere length: how the length makes a difference. Mol. Biol. Rep. **47**: 7181–7188. doi:10.1007/s11033-020-05551-y. PMID: 32876842.

Mahmoudi, A., Jamialahmadi, T., Johnston, T.P., and Sahebkar, A. 2022. Impact of fenofibrate on NAFLD/NASH: a genetic perspective. Drug Discov. Today, **27**: 2363–2372. doi:10.1016/j.drudis.2022.05.007. PMID:35569762.

Mahmoudi, A., Moallem, S.A., Johnston, T.P., and Sahebkar, A. 2022. Liver protective effect of fenofibrate in NASH/NAFLD animal models. PPAR Res. **2022**; Article ID 5805398 |. doi:10.1155/2022/5805398. PMID: 35754743.

Mikkola, H.K., and Orkin, S.H. 2006. The journey of developing hematopoietic stem cells. Development, **133**: 3733–3744. doi:10.1242/dev.02568. PMID: 16968814.

Muhammad, N., Ibrahim, K., Ndhlala, A., and Erlwanger, K. 2020. *Moringa oleifera* Lam. prevents the development of high fructose diet-induced fatty liver. S. Afr. J. Bot. **129**: 32–39. doi:10.1016/j.sajb.2018.12.003.

Nawrot, T.S., Staessen, J.A., Gardner, J.P., and Aviv, A. 2004. Telomere length and possible link to X chromosome. Lancet North Am. Ed. **363**: 507–510. doi:10.1016/S0140-6736(04)15535-9.

Patel, M.S., and Srinivasan, M. 2010. Metabolic programming due to alterations in nutrition in the immediate postnatal period. J. Nutr. **140**: 658–661. doi:10.3945/jn.109.110155. PMID: 20107149.

Pedersen, S.B., Kristensen, K., Hermann, P.A., Katzenellenbogen, J.A., and Richelsen, B. 2004. Estrogen controls lipolysis by up-regulating α2A-adrenergic receptors directly in human adipose tissue through the estrogen receptor α. Implications for the female fat distribution. J. Clin. Endocrinol. Metab. **89**: 1869–1878. doi:10.1210/jc.2003-031327.

Pepin, A., Stanhope, K.L., and Imbeault, P. 2019. Are fruit juices healthier than sugar-sweetened beverages? A review. Nutrients, **11**: 1006. doi:10.3390/nu11051006. PMID: 31052523.

Pérez-Corredor, P., Gutiérrez-Vargas, J., Ciro-Ramírez, L., Balcazar, N., and Cardona-Gómez, G. 2022. High fructose diet-induced obesity worsens post-ischemic brain injury in the hippocampus of female rats. Nutr. Neurosci. **25**: 122–136. doi:10.1080/1028415X.2020.1724453. PMID: 32116157.

Raymond, A.R., Norton, G.R., Sareli, P., Woodiwiss, A.J., and Brooksbank, R.L. 2013. Relationship between average leucocyte telomere length and the presence or severity of idiopathic dilated cardiomyopathy in black Africans. Eur. J. Heart Fail. **15**: 54–60. doi:10.1093/eurjhf/hfs147. PMID: 23035035.

Reynolds, C.M., Gray, C., Li, M., Segovia, S.A., and Vickers, M.H. 2015. Early life nutrition and energy balance disorders in offspring in later life. Nutrients, **7**: 8090–8111. doi:10.3390/nu7095384. PMID: 26402696.

Sclafani, A., Hertwig, H., Vigorito, M., and Feigin, M.B. 1987. Sex differences in polysaccharide and sugar preferences in rats. Neurosci. Biobehav. Rev. **11**: 241–225. doi:10.1016/S0149-7634(87)80032-5.

Shah, A., Rader, D.J., and Millar, J.S. 2010. The effect of PPAR-α agonism on apolipoprotein metabolism in humans. Atherosclerosis, **210**: 35–40. doi:10.1016/j.atherosclerosis.2009.11.010. PMID: 20005515.

Stephenson, E.J., Stayton, A.S., Sethuraman, A., Rao, P.K., Meyer, A., Gomes, C.K., et al. 2022. Chronic intake of high dietary sucrose induces sexually dimorphic metabolic adaptations in mouse liver and adipose tissue. Nat. Commun. **13**, Article number: 6062, 1–19. doi:10.1038/s41467-022-33840-6. PMID: 34983933.

Sutanto, S.S.I., Mclennan, S.V., Keech, A.C., and Twigg, S.M. 2019. Shortening of telomere length by metabolic factors in diabetes: protective effects of fenofibrate. J. Cell Commun. Signaling, **13**: 523–530. doi:10.1007/s12079-019-00521-x. PMID: 31203557.

Teixeira, M.Z. 2021. Telomere length: biological marker of cellular vitality, aging, and health-disease process. Rev. Assoc. Med. Bras. **67**: 173–177. doi:10.1590/1806-9282.67.02.20200655.

Tellechea, M., Gianotti, T.F., Alvariñas, J., González, C.D., Sookoian, S., and Pirola, C.J. 2015. Telomere length in the two extremes of abnormal fetal growth and the programming effect of maternal arterial hypertension. Sci. Rep. **5**: 7869–7876. doi:10.1038/srep07869. PMID: 25598199.

Van Lieshout, S.H., Sparks, A.M., Bretman, A., Newman, C., Buesching, C.D., Burke, T., et al. 2021. Estimation of environmental, genetic and parental age at conception effects on telomere length in a wild mammal. J. Evol. Biol., **34**: 296–308. doi:10.1111/jeb.13728. PMID: 33113164.

Vedder, O., Moiron, M., Bichet, C., Bauch, C., Verhulst, S., Becker, P.H., and Bouwhuis, S. 2021. Telomere length is heritable and genetically correlated with lifespan in a wild bird. Mol. Ecol. **31**: 6297–6307. doi:10.1111/mec.15807. PMID: 33460462.

Wallace, M., and Metallo, C.M. 2020. Tracing insights into de novo lipogenesis in liver and adipose tissues. Semin. Cell Dev. Biol. **108**: 65–71. doi:10.1016/j.semcdb.2020.02.012.

Wang, Z., and Wu, X. 2021. Abnormal function of telomere protein TRF2 induces cell mutation and the effects of environmental tumor–promoting factors. Oncol. Rep. **46**: 1–20. doi:10.3892/or.2021.8135.

Wojcicki, J.M., Heyman, M.B., Elwan, D., Lin, J., Blackburn, E., and Epel, E. 2016. Early exclusive breastfeeding is associated with longer telomeres in Latino preschool children. Am. J. Clin. Nutr. **104**: 397–405. doi:10.3945/ajcn.115.115428. PMID: 27440083.

Wong, K.K. 2021. DNMT1: a key drug target in triple-negative breast cancer. Semin. Cancer Biol. **72**: 198–213. doi:10.1016/j.semcancer.2020.05.010.

Xargay-Torrent, S., Mas-Parés, B., Carreras-Badosa, G., Lizárraga-Mollinedo, E., Tibau, J., Reixach, J., et al. 2022. Metabolic programming in the offspring after gestational overfeeding in the mother: toward neonatal rescuing with metformin in a swine model. Int. J. Obes. **46**: 1018–1026. doi:10.1038/s41366-022-01076-5. PMID: 35091671.

Zhao, S., Jang, C., Liu, J., Uehara, K., Gilbert, M., Izzo, L., et al. 2020. Dietary fructose feeds hepatic lipogenesis via microbiota-derived acetate. Nature, **579**: 586–591. doi:10.1038/s41586-020-2101-7. PMID: 32214246.

Zhu, Z., Cao, F., and Li, X. 2019. Epigenetic programming and fetal metabolic programming. Front. Endocrinol. **10**: 764. doi:10.3389/fendo.2019.00764. PMID: 31849831.